Graph Link Invariants of Isolated Singularities of Holomorphic Vector Fields in $\mathbb{C}^2$ I

Nobuatsu OKA

(Communicated by K. Akao)

1. Introduction.

The study of holomorphic vector fields (or a complex one dimensional foliation) has a long history (see [1], [3], [7] and [19]). There are already many studies in this field. Especially, in the last decades, Camacho, Neto and Sad have been studying actively and shed light on the geometrical and topological aspects of holomorphic vector fields (see [2], [4], [6] and [13]). In 1978, Camacho exhibited several topological invariants of holomorphic vector field Z defined on an open neighborhood of an isolated singular point $o = (0, 0)$ of $\mathbb{C}^2$ when the vector field Z has a non-zero linear term in the Taylor development at o. In 1984, Camacho and Sad obtained a more general topological invariant near a singularity of a holomorphic vector field Z in $\mathbb{C}^n$ ($n \geq 2$) (see [4] and also [5]). In their paper [4], they defined the *Milnor number* μ of a vector field Z at its singularity $o \in \mathbb{C}^n$ as $\mu = \dim_{\mathbb{C}} \mathcal{O}_n / I(Z_1, Z_2, \cdots, Z_n)$, where $\mathcal{O}_n$ means the ring of all germs of the holomorphic functions defined on some neighborhood of $o \in \mathbb{C}^n$ and $I(Z_1, \cdots, Z_n)$ means the ideal generated by the germs at $o \in \mathbb{C}^n$ of the coordinate functions of Z. When $o \in \mathbb{C}^n$ is an isolated singularity of Z, they asserted that the number μ coincides with the topological degree of the Gauss mapping induced from a real vector field constructed by Z in a small $(2N-1)$-sphere around $o \in \mathbb{C}^n$ ($n \geq 2$), and obtained that the Milnor number μ of Z is a topological invariant of the holomorphic foliation F_Z induced from the vector field Z (the foliation F_Z is the integral of the holomorphic vector field Z defined on an open neighborhood U of $o \in \mathbb{C}^n$). Simultaneously, they studied *generalized curves*, the special vector fields on $\mathbb{C}^2$ whose singularities become non-zero simple singularities after performing several blowing-ups. And also they obtained that the algebraic multiplicity of a generalized curve is a topological invariant, where the algebraic multiplicity means the degree of the first non zero term in the Taylor development of the vector field at o.

On the other hand, W. D. Neumann and W. Eisenbud studied plane curve

---

singularities by using powerful tools, i.e., splice diagrams of multi-links (see [8], [15] and [16]). Also Lee Rudolph and W. D. Neumann developed a new invariant of a real vector field around an isolated singularity from the view points of the link theory and the multi-link theory (see [17]). It seems that Neumann's techniques are also very useful to study the topological invariants near an isolated singularity of the generalized curve.

Thus we start to study relationships between topological invariants near a singularity of a generalized curve and splice diagrams or the multi-links. Firstly, we pay our attentions to the separatrices which are the leaves passing through an isolated singularity in C^2. After performing desingularizations of a vector field Z with a singularity at $o \in C^2$, a neighborhood changes into a certain real 4-submanifold (called a plumbed 4-manifold) whose boundary is a 3-sphere of the connected sum $kCP^2 \# C^2$ of k copies of CP^2's and C^2. Now the intersection of the above separatrices and the boundary of the plumbed 4-manifold can be considered as a graph multi-links. In this paper we define a plumbing diagram for a given generalized curve Z. Our plumbing diagram is analogous to the one for a plane curve singularity. We denote this diagram by P_Z. As we mention in §2, the diagram P_Z consists of the vertex denoted by a black dot ●, the special vertex (a so called *critical component*) denoted by ◎, the line which connects two vertices, and the arrowhead line which represents a separatrix. By using plumbing diagrams which have no critical components we can obtain a graph called the splice diagram (see Figure 2). The splice diagram is a certain decorated tree. The decorations consist of an integer weight at each end of some edge and an integer weight at certain vertices called *arrowhead vertices*. The former is called the *edge weight* and the latter the *vertex weight*. In general, this diagram represents a graph link in a homology 3-sphere and arrowhead vertices correspond to components of the link. The vertex weights define the orientation and the multiplicity of the components of the given graph link. In our cases, the splice diagrams represent multiple links which are intersections between the separatrices and the boundary of the plumbed 4-manifold. We denote this diagram by Γ_Z, which enables us to calculate the Thurston norm and the Alexander polynomials. So, for a given generalized curve Z, we define the one variable Alexander polynomial Δ_Z which is induced from the splice diagram Γ_Z of which all vertex weights are $+1$, and denote the cardinal number of critical components of P_Z by n_Z. Here n_Z may be zero. Now we consider the pair (Δ_Z, n_Z). When the splice diagram Γ_Z has no arrowhead vertices, we write (Δ_Z, n_Z) as $(\varnothing, n_Z)$, where the symbol $\varnothing$ means an empty set. Then we obtain the following theorem.

THEOREM A.   *Suppose that Z is a generalized curve with a singular point $o \in C^2$ and that Z' is any vector field topologically equivalent to Z around $o \in C^2$. Then Z' is also a generalized curve, and the pair (Δ_Z, n_Z) coincides with the pair $(\Delta_{Z'}, n_{Z'})$.*

As we mentioned before, a splice diagram represents a graph link. Especially, we consider the splice diagram Γ_Z of which all vertex weights are $+1$ induced from a vector field Z and the link L_Z represented by Γ_Z. Then we can define the Thurston norm of

the link L_Z. We will call this norm *the Thurston norm of the vector field Z*, and denote it by $\|Z\|$. If Γ_Z has no arrowhead vertices, we define its norm to be 0. It is clear that the value 0 is a topological invariant. Now we obtain the following main theorem.

THEOREM B. *Suppose that the holomorphic vector field Z which satisfies the condition $Z(o)=0$ is a generalized curve, and is defined on a neighborhood U of o in $\mathbf{C}^2$ which is homeomorphic to an open 4-ball. Then the Thurston norm $\|Z\|$ is a topological invariant of the vector field Z, that is, if a holomorphic vector field Z' is topologically equivalent to Z around $o \in \mathbf{C}^2$, then $\|Z'\| = \|Z\|$.*

REMARK. The Thurston norm of a generalized curve Z is an extension of the geometric (original) Milnor number in the case of the analytic curve. (See [12] for the definition of the original geometric Milnor number.) In fact, if Z is a Hamiltonian vector fields, (the Milnor number of Z)-1 is equal to the norm of Z (see §5). Our studies are motivated by this fact.

2. The definition of the plumbing diagram of the vector fields.

In this section, we introduce the concept of the plumbing diagram of the vector fields. Firstly, we state the blowing-up method. (For the details, we refer to [4] and [5]).

Let Z be a holomorphic vector field defined in an open set $U \subset \mathbf{C}^2$ with $Z(o)=0$. We assume that $o \in \mathbf{C}^2$ is the isolated singularity of Z in U. Suppose that the foliation F_Z is induced by the Pfaffian form $\omega = Z_2(x, y)dx - Z_1(x, y)dy = 0$, where $Z = Z_1(x, y)\partial/\partial x + Z_2(x, y)\partial/\partial y$, and F_Z is regular in $U - \{o\}$.

DEFINITION 1 ([5]). The singularity is said to be simple if the eigenvalues λ_1, λ_2 of $dZ(o)$ satisfy one of the conditions:
  (1) $\lambda_1 \lambda_2 \neq 0$, and $\lambda_1/\lambda_2 \notin \mathbf{Q}_+$ where $\mathbf{Q}_+ = \{x \in \mathbf{Q} \mid x > 0\}$,
  (2) $\lambda_1 = 0$ and $\lambda_2 \neq 0$.

The blow-up of $o \in \mathbf{C}^2$ consists of replacing o by a one dimensional projective line CP^1 considered as the set of limit directions at o. We introduce complex coordinates in $U^{(1)} = U - \{o\} \cup CP^1$ as follows: Any open subset of $U - \{o\}$ keeps its coordinates; in order to cover CP^1 we use two charts, $\phi_1 : V_1 \times \mathbf{C}^1 \to U - \{y=0\} \cup CP^1 - \{o\}$ and $\phi_2 : \mathbf{C}^1 \times V_2 \to U - \{x=0\} \cup CP^1 - \{\infty\}$ related by $\phi_2^{-1}\phi_1(x, t) = (t^{-1}, tx)$ for $t \neq 0$. These charts cover the neighborhoods of $CP^1 - \{\infty\}$ and $CP^1 - \{o\}$. The projection $\pi^{(1)} : U^1 \to U$ is given by $\pi^{(1)}(p) = p$ for $p \in U^1 - CP^1$ and $\pi^{(1)}(p) = 0$ for $p \in CP^1$ and is written in these coordinates as $(x, t) \to (x, xt)$ and $(u, y) \to (uy, y)$ respectively. We now lift the foliation F_Z to $U^{(1)}$. Z is written as

$$\dot{x} = a_v(x, y) + R_1(x, y),$$
$$\dot{y} = b_v(x, y) + R_2(x, y),$$

where $(a_v(x, y), b_v(x, y))$ is the first non zero jet of Z at $o \in \mathbf{C}^2$ and the positive integer $v = v_Z \in \mathbf{N}$ is called the *algebraic multiplicity* of Z (or F_Z) at the singularity o. Then we have the following equations for π^*Z:

(∗)
$$\dot{x} = x^v(a_v(1, t) + x R_1'(x, t)),$$
$$\dot{t} = x^{v-1}(b_v(1, t) - t a_v(1, t)) + x^v(R_2'(x, t) - t R_1'(x, t));$$

$$\dot{u} = y^{v-1}(a_v(u, 1) - u b_v(u, 1)) + y^v(R_1''(u, y) - u R_2''(u, y)),$$
$$\dot{y} = y^v(b_v(u, 1) + y R_2''(u, y)),$$

where $R_1'(x, t)$, $R_2'(x, t)$, $R_1''(u, y)$ and $R_2''(u, y)$ are higher terms in the Taylor developments at o. Then all the points of CP^1 are the singularities of π^*Z. To desingularize the singularities we have two ways (1) and (2) below (see [4]).

(1)   Nondicritical case. Suppose that $b_v(1, t) - t a_v(1, t) \neq 0$. Dividing (∗) by x^{v-1} we get

(∗∗)
$$\dot{x} = x(a_v(1, t) + x R_1'(x, t)),$$
$$\dot{t} = b_v(1, t) - t a_v(1, t) + x(R_2'(x, t) - t R_1'(x, t)).$$

The expression found in the other coordinate system fits with (∗∗), and we can define a foliation $F_Z^{(1)}$ in $U^{(1)}$ having CP^1 as an invariant set. More precisely, some of isolated singularities are given by the roots of $b_v(1, t) - t a_v(1, t) = 0$ and CP^1 is a leaf of $F_Z^{(1)}$. We can see that $F_Z^{(1)}$ and π^*F_Z coincide outside CP^1.

(2)   Dicritical case. Suppose that $b_v(1, t) - t a_v(1, t) \equiv 0$. After dividing (∗) by x^v we find

$$\dot{x} = a_v(1, t) + x R_1'(x, t),$$
$$\dot{t} = R_2'(x, t) - t R_1'(x, t).$$

In this case, we also see that $F_Z^{(1)}$ and π^*F_Z coincide outside CP^1, but the projective line CP^1 is not an invariant set. The foliation $F_Z^{(1)}$ is transverse to CP^1 except at a finite number of points (the roots of the equation $a_v(1, t) = 0$, which may or may not be singularities).

It is important to notice that foliations of both cases are locally given by analytic expressions. Therefore, we can repeat the process at any singular point in $F_Z^{(1)}$. The process can be applied repeatedly. After kth blow-up, we have a foliation $F^{(k)}$ defined in a neighborhood $U^{(k)}$ of a union $CP^{1(k)}$ of projective lines with normal crossings and we have a proper analytic projection $\pi^{(k)} : U^{(k)} - CP^{1(k)} \to U - \{o\}$ which is an isomorphism between the foliations $F^{(k)}$ and F_Z. We will write $(U^{(k)}, \pi^{(k)}, CP^{1(k)}, F^{(k)})$ to denote a kth blow-up of Z at $o \in \mathbf{C}^2$, where $\pi^{(k)}$ will be called its projection and $CP^{1(k)}$ its *divisor*.

The Desingularization Theorem for vector fields ([1], [10], [19] and [20]) asserts that all singularities become simple after a finite times of blow-ups. Therefore, if we start the procedure at $o \in \mathbf{C}^2$ and if we do not need to perform the further explosions for all simple singularities after kth blow-up, we call the desingularization of Z at o for this situation. (See Lemma 3 in §3 and Theorem 5 in [4].) And also the situation defines uniquely the blow-ups $(U^{(k)}, \pi^{(k)}, P^{(k)}, F_Z^{(k)})$ as the desingularization of Z at o. An alternative notation we use for desingularization of Z is (U_Z, π_Z, P_Z, F_Z).

DEFINITION 2 ([4]).   The vector field Z is a *generalized curve* if F_Z in the desingularization of Z has no singularities with zero eigenvalues.

DEFINITION 3 ([4]).   The divisor is a union of embedded projective lines intersecting transversely at a finite number of points called *corners*.

DEFINITION 4 ([4]).   A separatrix of Z is a connected integral curve V of Z such that $\overline{V} = V \cup \{o\}$.

Now we represent the desingularization of a generalized curve Z at 0 in a graphic form as in Figure 1; we will represent a separatrix by an arrowhead line $\uparrow$, an invariant component of the divisor by a straight line $|$, and a non-invariant component of the divisor by a symbol $\|$. We exclude leaves which do not intersect the divisor and those which intersect a non-invariant component of the divisor from the last stage of desingularizations, because these leaves do not relate to simple singularities of the final stage of the desingularizations. We call this graphic form the *final resolution picture*.

Also we define a plumbing diagram of a vector field in which we have also written the self-intersection numbers of the components of the divisor as in Figure 1. This graph also represents the final stage of the desingularization of a generalized curve and is a dual graph of the final resolution picture. The symbol "$\rightarrow$" means the separatrix of the vector field. We call this vertex an arrowhead vertex. The symbol "$\bullet$" denotes an invariant component of the divisor in the desingularizations, and the symbol "$\odot$" denotes a non-invariant component of the divisor. The edges of the plumbing diagram represent the normal crossing points. Here, the normal crossing point means a corner or an intersection point between the divisor and a separatrix of a simple singularity in the last stage of the resolution. Thus we exclude all intersection points in non-invariant divisors of the final stage of the resolution from our normal crossing points.

DEFINITION 5.   We call a vertex corresponding to the non-invariant component of the divisor of the final resolution picture a *non-invariant vertex* of the plumbing diagram.

Each component CP_i of the divisor has the self-intersection number $CP_i \cdot CP_i = -1$ at first, since it appears as an exceptional curve (cf. [9]). And whenever a singular point is blown-up on it, the self-intersection number decreases by 1. Then we put the absolute value of self-intersection number on every vertex. We call this value a *vertex weight of*

plumbing diagram. Now we will present some examples.

EXAMPLE 1 (critical case).

$$\dot{x} = x^4 y$$
$$\dot{y} = x^9 + y^4 + 2x^3 y^2$$
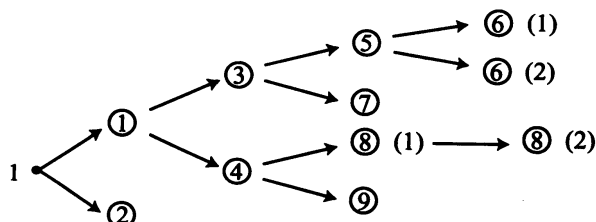
Flow chart of computations

① $(x, y) \rightarrow (x, xt_1)$

$$\dot{x} = x^2 t_1$$
$$\dot{t}_1 = x^5 + t_1^4 + x t_1^2$$

② $(x, y) \rightarrow (y u_1, y)$

$$\dot{y} = y + y^6 u_1^9 + 2y^2 u_1^3$$
$$\dot{u}_1 = -u_1 - y u_1^4 - u_1^{10} y^5$$

③ $(x, t_1) \rightarrow (x, x t_2)$

$$\dot{x} = t_2$$
$$\dot{t}_2 = x + t_2^4$$

④ $(x, t_1) \rightarrow (t_1 u_2, t_1)$

$$\dot{t}_1 = t_1 + u_2 + t_1^2 u_2^5$$
$$\dot{u}_2 = -u_2 - t_1 u_2^6$$

⑤ $(x, t_2) \rightarrow (x, x t_3)$

$$\dot{x} = t_3 x$$
$$\dot{t}_3 = 1 + t_3^4 x^3 - t_3^2$$

The point $(x, t_3) = (0, 0)$ is non-singular.

⑥ (1) $(x, t_3 - 1) \rightarrow (x, t_3)$

$$\dot{x} = x + t_3 x$$
$$\dot{t}_3 = -2t_3 + \text{(higher order)}$$

⑥ (2) $(x, t_3 + 1) \rightarrow (x, t_3)$

$$\dot{x} = -x + t_3 x$$
$$\dot{t}_3 = 2t_3 + \text{(higher oder)}$$

⑦ $(x, t_2) \rightarrow (t_2 u_3, t_2)$

$$\dot{t}_2 = t_2 u_3 + t_2^4$$
$$\dot{u}_3 = -u_3^2 - t_2^3 u_3 + 1$$

The point $(t_2, u_3) = (0, 0)$ is non-singular.

⑧ (1) $(t_1, u_2) \rightarrow (u_2 t_4, u_2)$

$$\dot{u}_2 = -u_2 - u_2^7 t_4$$
$$\dot{t}_4 = 2t_4 + 1 + 2u_2^6 t_4^2$$

The point $(t_4, u_2) = (0, 0)$ is non-singular.

⑧ (2) $(u_2, t_4 + 1/2) \rightarrow (u_2, t_4)$

$$\dot{u}_2 = -u_2 - u_2^7 (t_4 - 1/2)$$
$$\dot{t}_4 = 2t_4 + \text{(higher order)}$$

⑨ $(t_1, u_2) \rightarrow (t_1, t_1 u_4)$

$$\dot{t}_1 = t_1 + u_4 t_1 + t_1^7 u_4^5$$
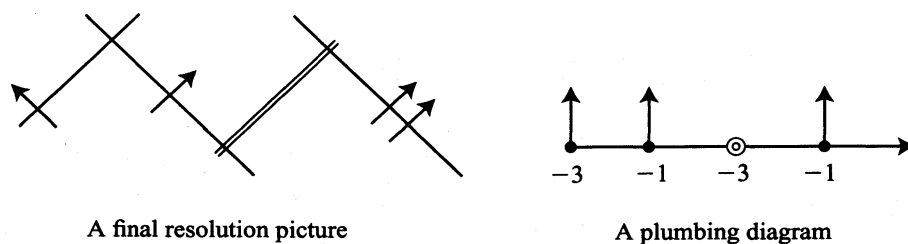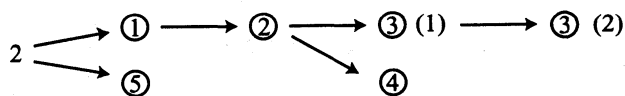$$\dot{u}_4 = -2u_4 - u_4^2 - 2u_4^6 t_1^6$$

See Figure 1 (cf. [4]).

A final resolution picture

A plumbing diagram

FIGURE 1

EXAMPLE 2.

$$\dot{x} = -3y^2$$
$$\dot{y} = 2x$$

Flow chart of computations

① $(x, y) \rightarrow (yu_1, y)$

$\dot{y} = 2yu_1$

$\dot{u}_1 = -3y - 2u_1^2$

② $(y, u_1) \rightarrow (u_1 t_2, u_1)$

$\dot{t}_2 = 4t_2 u_1 + 3t_2^2$

$\dot{u}_1 = -2u_1^2 - 3u_1 t_2$

③ (1) $(u_1, t_2) \rightarrow (u_1, u_1 t_3)$

$\dot{t}_3 = 6t_3 + 6t_3^2$

$\dot{u}_1 = -2u_1 - 3u_1 t_3$

③ (2) $(u_1, t_3 + 1) \rightarrow (u_1, t_3)$

$\dot{t}_3 = -6t_3 + 6t_3^2$

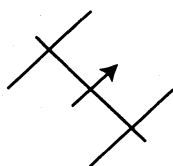$\dot{u}_1 = u_1 - 3u_1 t_3$

④ $(u_1, t_2) \rightarrow (t_2 u_3, t_2)$

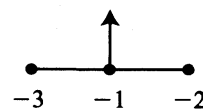$\dot{t}_2 = 3t_2 + 4t_2 u_3$

$\dot{u}_3 = -6u_3 - 6u_3^2$

⑤ $(x, y) \rightarrow (x, xt_1)$

$\dot{x} = -3x^2 t_1^2$

$\dot{t}_1 = 2 + 3t_1^3 x$

A final resolution picture

A plumbing diagram

FIGURE 2

EXAMPLE 3.
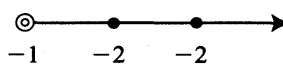
$$\dot{x} = 3x$$
$$\dot{y} = y$$

A plumbing diagram

FIGURE 3

EXAMPLE 4.

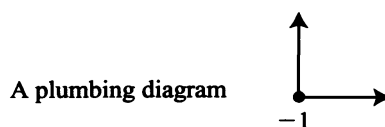$$\dot{x} = 3x$$
$$\dot{y} = -y$$

A plumbing diagram

FIGURE 4

Observe that the nondicritical generalized curve must have at most a finite number of separatrices.

There is a notion of minimality for plumbing diagrams, which is stated as follows.

DEFINITION 6 (Minimal plumbing diagram [8]). If a plumbing diagram does not contain any of the configurations on the left hand sides of part 1)–4) of Figure 5, then we call it *minimal plumbing diagram*.

1)

or

2)

3)

or

4)

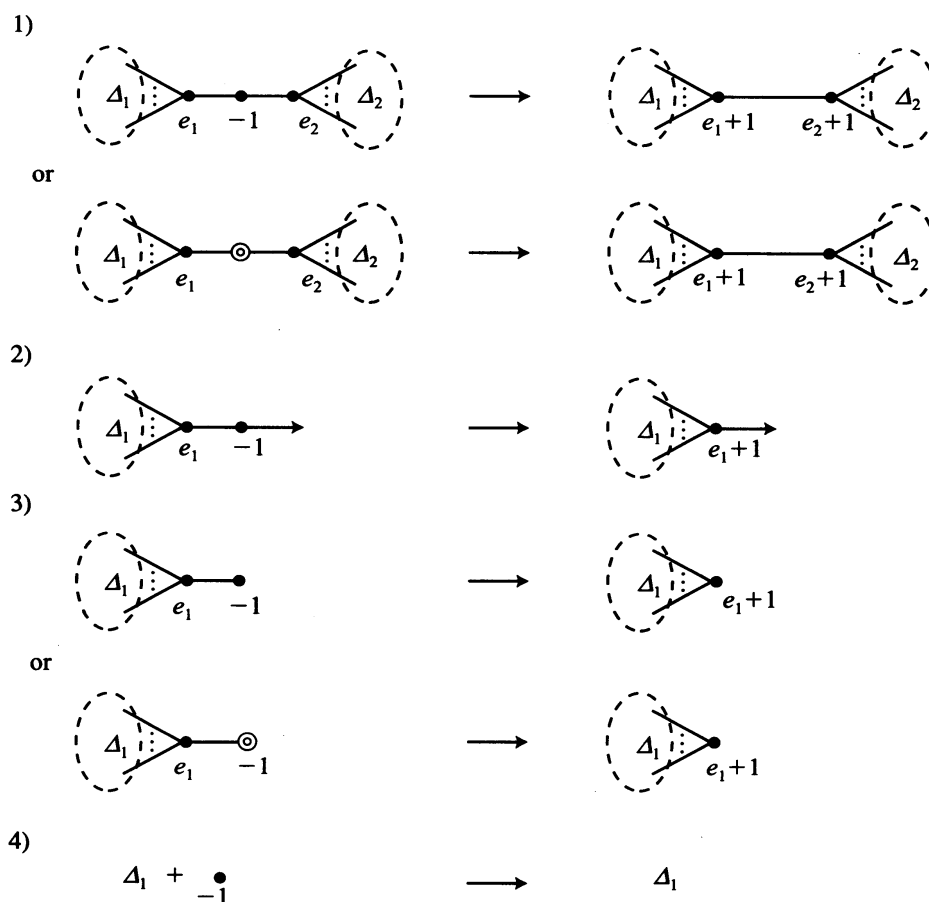$$\Delta_1 + \underset{-1}{\bullet} \longrightarrow \Delta_1$$

FIGURE 5

In the diagrams 1)–4) of Figure 5, the left hand side is equivalent to the right hand side. Therefore, if the left hand side diagram appears in a plumbing diagram, then it can be replaced by the right hand side diagram.

To prove main theorems we need the concepts of splicing of two graph links, splice diagrams and their minimality. First we state the notion of splicing of two graph links and splice diagrams and then explain about the notion of minimality.

DEFINITION 7 ([8]). Let $L=(\Sigma, K)$ and $L'=(\Sigma', K')$ be links and choose components $S \subset K$ and $S' \subset K'$. Let $N(S)$ and $N(S')$ be tubular neighborhoods and $M, L \subset \partial N(S)$ and $M', L' \subset \partial N(S')$ be standard meridians and longitudes, and construct $\Sigma'' = (\Sigma - \text{int } N(S)) \cup (\Sigma' - \text{int } N(S'))$ pasting along boundaries by matching M to L' and L to M'. Then the link $(\Sigma'', (K-S) \cup (K'-S'))$ is called a splice of L and L' along S and S' and is denoted by $L\text{———}L'$ or $L_{\overline{S}\overline{S'}}L'$, where both manifolds Σ and Σ' are homology spheres.

It is easily checked that the manifold Σ'' is a homology sphere. We describe a multi-link which is first introduced by Neumann. It is a natural extension of the concept of link. Let $(\Sigma, \mathbf{K})$ be an unoriented link and $L=(\Sigma, S_1 \cup \cdots \cup S_n)$ be a link obtained by orienting $(\Sigma, \mathbf{K})$. By a *multi-link on* $(\Sigma, \mathbf{K})$ we mean L together with integer multiplicity m_i associated to each component S_i, with a convention that a component S_i with multiplicity m_i means the same link component as $-S_i$ (S_i with reversed orientation with multiplicity $-m_i$). We write the multi-link $L(m_1, \cdots, m_n) = (\Sigma, m_1 S_1 \cup \cdots \cup m_n S_n)$. A link is thus simply a multi-link with all multiplicities ± 1.

A multi-link on $(\Sigma, \mathbf{K})$ as above determines an integral cohomology class $\underline{m} \in H^1(\Sigma - \mathbf{K}) = H_1(\Sigma - \mathbf{K})^*$ as follows: $\underline{m}$ evaluated on a 1-cycle S is the linking number; i.e.,

$$\underline{m}(S) = \text{link}(m_1 S_1 + \cdots + m_n S_n, S) = \sum m_i \text{link}(S_i, S) .$$

By Alexander duality the n linear forms $\text{link}(S_i, -) \in H_1(\Sigma - \mathbf{K})$ $(i=1, \cdots, n)$ are identified with a base of $\mathbf{Z}^n$. Then we can write $\underline{m} = (m_1, \cdots, m_n)$. We may also write $L(\underline{m})$ for $L(m_1, \cdots, m_n)$. Given $\underline{m}$ and a link $(\Sigma, \mathbf{K})$, one computes m_i by $m_i = \underline{m}(M_i)$, where M_i is a standard oriented meridian of an oriented link component S_i.

Now we show some examples of splice diagrams. Recall that the splice diagram is a tree having edge weights and vertex weights. Also some of the vertices of the diagram are drawn as arrowheads, which correspond to components of the link. We call the vertices *arrowhead vertices*. For example if we construct a torus link by iterated cabling,
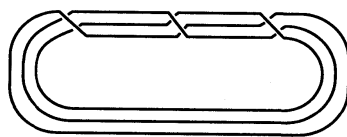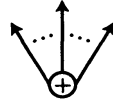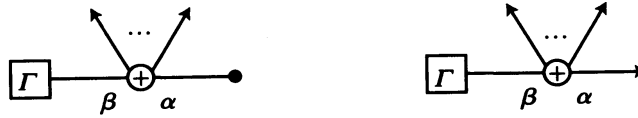

FIGURE 6. *n*-Hopf link ($n=3$)

we will start from the n-component Hopf link $H_n = (S^3, K_1 \cup \cdots \cup K_n)$ consisting of n fibers of the Hopf fibration. We represent this link by the splice diagram with n arrowheads:

If $\boxed{\Gamma} \to$ is a splice diagram for a link L and the indicated arrowhead corresponds to a component K, then each of the diagrams

is the result of (α, β) cabling operation to L; namely either by replacing component K or adding d-parallel (α, β) cables on K. Thus we can construct a splice diagram for any toral link. The splice diagram
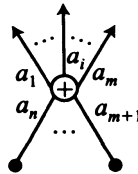
represents the Seifert link $(\pm \Sigma(a_1, a_2, \cdots, a_n), S_1 \cup \cdots \cup S_n)$.

DEFINITION 8 (*Minimal splice diagram* [8]). *Minimal splice diagram* is a splice diagram which does not contain any of the configurations on the left hand sides of part 1)-4) of the following ($\approx$ means an equivalence):

1)

$$\approx \qquad \Gamma(\underline{m}_1) \text{——} \Gamma(\varepsilon \underline{m}_2)$$
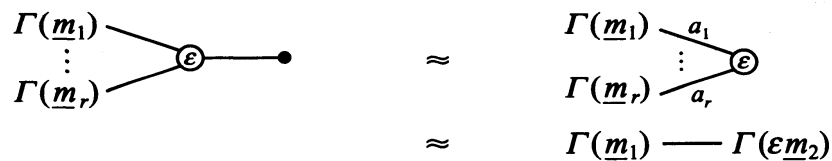
where ε $(= \pm)$ is two different orientations, and m_i $(1 \leq i \leq r)$ means the multiplicity of the link, and $\Gamma(m_i)$ represents a piece of a splice diagram.

2)

3) $\Gamma(\underline{m})$ + •———• (disjoint union) $\approx$ $\Gamma(\underline{m})$

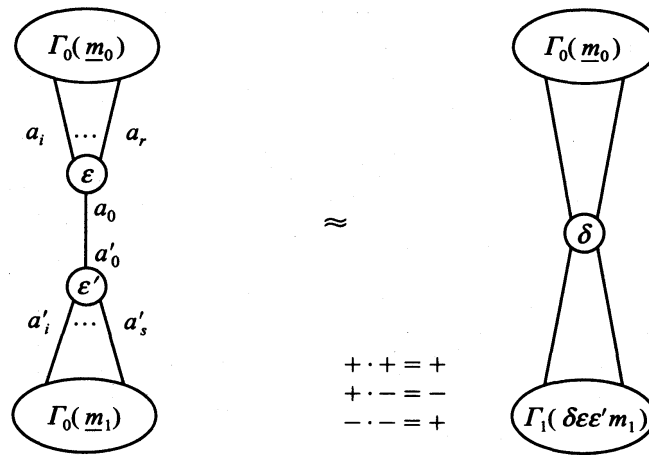4) If $a_0 a'_0 = \varepsilon\varepsilon' a_1 \cdots a_r a'_1 \cdots a'_s$, then

FIGURE 7

where $\delta = \pm 1$ is chosen so that

$$a_0 = \delta\varepsilon a'_1 \cdots a'_s, \qquad a'_0 = \delta\varepsilon' a_1 \cdots a_r.$$

For details of the splice diagram, see [15], [16] and [8].

3. Preparations.

We prepare in this section several lemmas and theorems needed to prove the main theorems. Firstly, we describe some notations concerning the graph theory. When one endpoint of an edge of a graph coincides with the other endpoint of this edge, we call this edge a *loop*. A closed path which has more than two edges is called a *cycle* of a graph.

LEMMA 1. *Let P_Z be a plumbing diagram induced by the desingularization of a vector field Z, and let X be a plumbed 3-manifold which is the boundary of the plumbed 4-manifold Y corresponding to the above plumbing diagram P_Z. If the 3-manifold X is a rational homology sphere, then P_Z is a tree.*

PROOF. Since Y is of the same homotopy type as the divisor and $H_1(X; \mathbf{Q}) = 0$, we see that $H_1(Y; \mathbf{Q}) = 0$ by using the following exact sequence:

$$\to H_1(X; \mathbf{Q}) \to H_1(Y; \mathbf{Q}) \to H_1(Y, X; \mathbf{Q}) \to H_0(X; \mathbf{Q}) \to$$
$$\overset{\shortparallel\wr}{H^3(Y; \mathbf{Q}) = 0}$$

Each component of the divisor is an embedded 2-sphere, and hence the diagram P_Z contains no loop. If P_Z is a cycle (see Figure 8), then doing CW-complex configuration

on each component of the divisor represented by the final resolution picture like Figure 9 (a) and (b), we can compute that $H_1(Y, \mathbf{Q}) \neq 0$. In the general case as in Figure 10, since the intersection points of the two complex projective line CP^1 are zero dimensional CW-complexes, we have also $H_1(Y, \mathbf{Q}) \neq 0$ by using Mayer-Vietoris exact sequence. This contradicts $H_1(Y, \mathbf{Q}) = 0$. Thus the final resolution picture has no cycles and the corresponding plumbing diagram also has no cycles and no loops, in other words, P_Z is a tree.
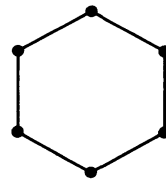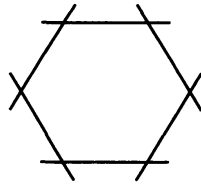

FIGURE 8.   A final resolution picture and a plumbing diagram corresponding to it.

(a)   (b)
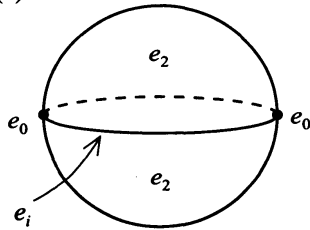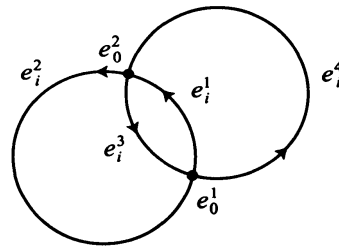
O denotes a component of a divisor.

FIGURE 9
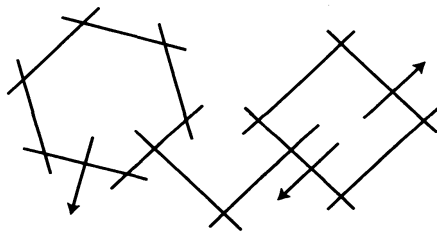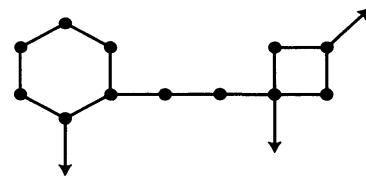
A final resolution picture   Corresponding plumbing diagram

FIGURE 10

REMARK.   In general, there exist some examples of the plumbing diagram having a loop. But these plumbing diagrams can not be induced from a desingularization of vector fields. To check it see Figure 11 and see [14]. (In Figure 11, the left plumbing diagram and the right one represent the same plumbed 3-manifold. The symbol "—"

on the edges of the left graphs means an edge sign. For the definition of this edge sign, see [14].)

FIGURE 11

LEMMA 2. *Let $A(P_Z)$ be an intersection form induced from a plumbing diagram P_Z of a generalized curve Z. Then $\det(A(P_Z)) = \pm 1$.*

PROOF. The plumbed 3-manifold is the boundary of a plumbed 4-manifold which is induced by the desingularizations of the vector field Z. Hence the plumbed 3-manifold is a 3-sphere. Let U be a neighborhood of isolated singularity of Z in $\mathbf{C}^2$ such that $\partial U = S^3$. Let $(U_Z, CP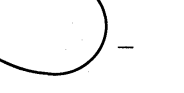_Z^1, \pi_Z, F_Z)$ be a desingularization of Z. Let the plumbed 3-manifold X be the boundary of a plumbed 4-manifold Y. Since $\pi_Z^{-1}(\partial U) = \pi_Z^{-1}(S^3) = S^3 = \partial U_Z$, we have $H_1(Y, \mathbf{Z}) = 0$ by the following exact sequence.

$$0 \to H_2(X, \mathbf{Z}) \to H_2(Y, \mathbf{Z}) \to H_2(Y, X, \mathbf{Z}) \to H_1(X, \mathbf{Z}) \to H_1(Y, \mathbf{Z}) \to$$

$$\begin{array}{ccc} \| \wr & \| & \| \\ H^2(Y, \mathbf{Z}) & \{o\} & \{o\} \\ \| \wr & & \\ \operatorname{Hom}(H_2(Y), \mathbf{Z}) & & \end{array}$$

Here ψ denotes the correlation associated with the quadratic form which is induced by the intersection number of 2-cycles of $H_2(Y, \mathbf{Z})$ and is represented by the matrix $A(P_Z)$. (See [9]). Using the above exact sequence, we see that cokernel $\psi = 0$, and hence $UA(P_Z)V = E$, where U and V are unimodular matrices and E denotes the identity matrix. Thus $\det(A(P_Z)) = \pm 1$.

DEFINITION 9 ([4]). Let Z be a vector field defined on a neighborhood of $p \in \mathbf{C}^2$ and let S be a smooth curve through p which is not invariant under Z. (x, y) denotes the local coordinates with $p = (0, 0)$ and $S = \{(x, 0)\}$. Let $\dot{x} = a(x, y)$, $\dot{y} = b(x, y)$ be the equation for Z in this coordinate system. We define the order of tangency of Z with S

as the multiplicity of $0 \in \mathbf{C}$ as a root of $b(x, 0) = 0$. We denote it by $\eta_Z(p, S)$. (The case $\eta_Z(p, S) = 0$ is allowed.) If F is the foliation induced by Z, then we write $\eta_F(p, S)$ instead of $\eta_Z(p, S)$.

If a vector field is a degenerate generalized curve, the next Lemma 3 and Theorem 1 in [4] guarantee that all separatrices intersect transversely with the divisor.

LEMMA 3 ([4]). *Let F be a foliation defined in a neighborhood of $p \in \mathbf{C}^2$ with algebraic multiplicity v. Let S be a smooth curve through p and not invariant by F. Let $F^{(1)}$ be the foliation obtained by blowing-up at $p \in S$. Then*

(1) *If $p \in S$ is a nondicritical singularity, then $\eta_{F^{(1)}}(p, S) = \eta_F(p, S) - v$.*

(2) *If $p \in S$ is a dicritical singularity, then $\eta_{F^{(1)}}(p, S) = \eta_F(p, S) - (v + 1)$.*

(3) *If $p \in S$ is not a singularity and $\eta_F(p, S) \neq 0$ then $p(\in S)$ is a simple nondicritical singularity for $F^{(1)}$ with eigenvalues 1 and -1 and the equality: $\eta_{F^{(1)}}(p, S) = \eta_F(p, S)$ holds.*

We need the following lemma to prove the next theorem.

LEMMA 4 ([4]). *Suppose that*

$$\dot{x} = a_v(x, y) + a_{v+1}(x, y) + \cdots,$$
$$\dot{y} = b_v(x, y) + b_{v+1}(x, y) + \cdots$$

are differential equations for Z and $b_v(1, t) - t a_v(1, t) \equiv 0$. If P is the projective line and $F^{(1)}$ is the foliation which results from the explosion of $0 \in \mathbf{C}^2$, then $v - 1 = \sum \eta_{F^{(1)}}(p, P)$.

THEOREM 1 (Theorem 7 in [4]). *Let Z and Z' be vector fields with $Z(o) = Z'(o) = 0$ and having S_Z and $S_{Z'}$ as the sets of separatrices. Assume that Z is a generalized curve and that S_Z and $S_{Z'}$ have isomorphic desingularizations. Then $\mu(Z', o) \geq \mu(Z, o)$, and equality holds if and only if Z' is a generalized curve.*

PROOF. If the vector field Z is nondegenerate, the proof is given in [4]. So we assume that the vector field Z is degenerate. We prove by induction on the number of explosions that Z needs to become desingularized.

If Z needs just one explosion to become desingularized, then the divisor appearing in the first explosion is not invariant under Z. There is a fomula which relates the Milnor number of the vector field to the Milnor numbers of the singularities appearing in the first explosion, which is written as

$$\mu(Z, o) = v^2 + v - 1 + \sum \mu(F_Z^{(1)}, C) \tag{1}$$

where v is the algebraic multiplicity of Z. (We call this formula *the first blow-up formula of dicritical singularities* [11].) The separatrices S_Z intersect with the divisor $CP^{1(1)}$ transversely. Thus Z has no singularity in $CP^{1(1)}$. Since Z and Z' have the same desingularizations, the separatrices $S_{Z'}$ intersect with the divisor $CP^{1(1)'}$ transversely. By Lemma 4, we see that the algebraic multiplicity v of Z and the algebraic multiplicity v' of Z' are 1. Thus $\mu(Z, o) = \mu(Z', o) = 1$. Notice that Z' is also a generalized curve.

Assume that the theorem has been proved for singularities of Z whose set of separatrices need $m \in \mathbb{N}$ explosions to become desingularized. If Z' needs $m+1$ explosions to reach the final resolution picture, then explode Z once. We see that the singularities $P_1, P_2, \cdots, P_s$ in $F_Z^{(1)}$ are also singularities of $F_{Z'}^{(1)}$. Now we consider the next cases.

(1) Suppose that $CP^{1(1)}$ is an invariant divisor. By the same argument as in Theorem 4 in [4] we can get the conclusions.

(2) Suppose that $CP^{1(1)}$ is a non-invariant divisor. If Z' is a generalized curve, the points $P_1, \cdots, P_s$ are all singularities of Z'. Since Z and Z' have isomorphic desingularizations, Z and Z' have the same non-zero tangency points in $CP^{1(1)}$. Thus, by the induction hypothesis, Lemma 4 and the formula (1), we see $\mu(Z, o) = \mu(Z', o)$. Assume that Z' is not a generalized curve. Then the following two cases occur:

Case 1.   The points $P_1, \cdots, P_s$ are all the singularities of $F_Z^{(1)}$, and at least one of the vector field around them is not a generalized curve,

Case 2. $F_Z^{(1)}$ has additional singularities $P_{s+1}, P_{s+2}, \cdots, P_k$.

In the first case we have $\sum \mu(F_{Z'}^{(1)}, P_i) > \sum \mu(F_Z^{(1)}, P_i)$ by the induction hypothesis; in the second case the inequality $\sum \mu(F_{Z'}^{(1)}, P_i) > \sum \mu(F_Z^{(1)}, P_i)$ holds. Since $v_{Z'} \geqq v_Z$ from Lemma 4 we have $\mu(Z', o) > \mu(Z, o)$ from the formula (1).

The following three theorems play important roles in our proof of main theorems. Here we state them without proofs. See [4] and [5] for the proofs.

THEOREM 2 ([5]).   *For any holomorphic vector field Z, there exists a complex analytic subvariety which passes through $o \in \mathbb{C}^2$ and is invariant by Z. Especially, any separatrix of vector fields is a complex analytic subvariety.*

THEOREM 3 ([4]).   *Let Z be a generalized curve with an isolated singularity at $o \in \mathbb{C}^2$. If S is the set of separatrices of Z, then S and Z have the same desingularizations.*

THEOREM 4 ([4]).   *Let Z be a vector field and let $f = 0$ represent its separatrices. Suppose that a vector field Z_f is given by $\dot{x} = -\partial_y f(x, y)$, $\dot{y} = \partial_x(x, y)$, i.e., Z_f is a Hamiltonian system. If one has $\mu(Z, o) = \mu(Z_f, o)$, then the vector field Z must be a generalized curve where $\mu(Z, o)$ and $\mu(Z_f, o)$ are the Milnor numbers of the vector fields Z and Z_f respectively.*

We state some notations concerning the separatrices of a generalized curve. By Theorem 3, we can identify the separatrices with the set of analytic curves passing through the origin $o \in \mathbb{C}^2$. So we define the final resolution picture of separatrices by proceeding desingularizations of separatrices till all separatrices intersect transversely to the divisor. We can represent the last stage of desingularizations by a graphical form as in the case of the vector field. We call this graph a *final resolution picture of separatrices*. Also we call its dual graph a *plumbing diagram of separatrices*. Here, we represent separatrices by a symbol "↑" in a dual graph, and represent a divisor which intersects infinitely many separatrices by a symbol "◎". We omit arrowhead vertices which

represent separatrices intersecting to this divisor.

Theorem 5 and Lemma 5 are needed to compute the Thurston norm of a graph link represented by a splice diagram.

THEOREM 5 (Theorem 11.1 in [8]). *Let Γ be a splice diagram which has arrowheads $V_1, \cdots, V_n$ and remaining vertices $V_{n+1}, \cdots, V_k$, and $L(\Gamma(\underline{m})) = L(\Gamma(m_1, \cdots, m_n))$ be a multi-link on a graph link $L(\Gamma) = (\Sigma, S_1 \cup \cdots \cup S_n)$. Assume $L(\Gamma)$ is irreducible, and is not the unknot (S^3, S^1). Then the Thurston norm $\|\underline{m}\|$ of $L(\Gamma(\underline{m}))$ is given by*

$$\|\underline{m}\| = \sum_{j=n+1}^{k} (\delta_j - 2) |\underline{m}(S_j)| = \sum_{j=n+1}^{k} (\delta_j - 2) |m_i l_{1j} + \cdots + m_n l_{nj}|,$$

where δ_j denotes the degree of the j-th vertex in Γ (i.e., δ_j is the number of incident edges), and l_{ij} denotes the linking number of the vertices i and j. (See [8] for the definition of the linking number of two vertices of a splice diagram.)

PROOF. Suppose that $L(\Gamma)$ is a given graph link, then $L(\Gamma)$ can be represented by a splice diagram. Now we change this splice diagram to a minimal splice diagram by using procedures (1), (2), (3) and (4) in Definition 8. Because $L(\Gamma)$ is irreducible, its splice diagram does not have any configurations in the right hand sides of the operations (2) and (3) in Definition 8. If we check the way of calculation of the Thurston norm of graph links represented by splice diagrams, it is easy to see that the operations (1) and (4) do not alter the equations of this theorem (see [8]). Moreover, suppose that $L(\underline{m}) = L(\underline{m}')_{\overline{S'} \quad \overline{S''}} L(\underline{m}'')$ and that neither S' nor S'' is an unknot summand of the respective link L' or L''. (If one of S' and S'' is an unknot summand, then $L(\underline{m})$ is the disjoint sum of the multi links obtained by deleting S' and S'' from $L(\underline{m}')$ and $L(\underline{m}'')$.) Then a minimal Seifert surface for $L(\underline{m})$ can be obtained by pasting minimal Seifert surfaces for $L(\underline{m}')$ and $L(\underline{m}'')$ so that $\|\underline{m}\| = \|\underline{m}'\| + \|\underline{m}''\|$. (See Theorem 3.3 in [8]). Thus reversing orientation if necessary, we may assume that $\Gamma(\underline{m})$ is given as follows:
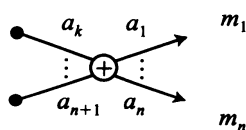
We number the central node $k+1$ and put $q_i = a_1 \cdots a_k / a_i$ for $1 \le i \le k$. Then the following equalities hold:

$$l_{ij} = q_i / a_j \quad \text{for} \quad 1 \le i \le n \text{ and } n+1 \le j \le k,$$
$$q_i \quad \text{for} \quad 1 \le i \le n \text{ and } j = k+1.$$

If we put $l = \sum q_i m_i$ then $\underline{m}(S_j) = 1/a_j$ for $n+1 \le j \le k$ and $\underline{m}(S_{k+1}) = l$. Thus it remains to prove that $\|m\| = (k - 2 - \sum 1/a_j) |l|$.

We use the analytic model

$$\Sigma = \Sigma(a_1, a_2, \cdots, a_n)$$
$$= \{z \in \mathbf{C}^n \mid a_{i1}z_1^{a_1} + \cdots + a_{in}z_n^{a_n} = 0 \text{ for } i = 1, 2, \cdots, n-2\} \cap S^{2n-1}$$

with the S^1-action $t(Z_1, \cdots, Z_n) = (t^{q_1}Z_1, t^{q_2}Z_2, \cdots, t^{q_n}Z_n)$, where $q_i = a_1 \cdots a_n/a_i$. Recall that $S_i = \{Z_i = 0\} \cap \Sigma$ in that model. Let $\Sigma' = \Sigma - (S^1 \cup \cdots \cup S^n)$. We claim that $\Lambda : \Sigma' \to S^1$ given by $\Lambda(Z_1, Z_2, \cdots, Z_n) = Z_1^{m_1}Z_2^{m_2} \cdots Z_n^{m_n}/|Z_1^{m_1} \cdots Z_n^{m_n}|$ is a representative for $\underline{m} \in H^1(\Sigma') = [\Sigma', S^1]$. Since $\Lambda = \Lambda_1^{m_1} \cdots \Lambda_n^{m_n}$ where $\Lambda_i(Z) = Z_i/|Z_i|$ and since the group structure in $[\Sigma', S^1]$ is induced from the group structure of S^1, we need only check our claim for each Λ_i. In fact, the canonical isomorphism;

$$H^1(\Sigma) = [\Sigma', S^1] \longrightarrow \operatorname{Hom}(H_1(\Sigma'), \mathbf{Z})$$
$$\cup \qquad\qquad\qquad \cup$$
$$[\Lambda_i] \longrightarrow \operatorname{link}(S_i, -)$$

satisfies the conditions

$$\{\arg \Lambda_i(f(2\pi)) - \arg \Lambda_i(f(0))\}/2\pi$$
$$= \{\arg(f^i(2\pi)/|f^i(2\pi)|) - \arg(f^i(0)/|f^i(0)|)\}/2\pi$$
$$= \delta_{ik} = \operatorname{link}(S_i, M_k) .$$

Here M_k denotes the meridian of S_k in $H_1(\Sigma')$ which is represented by the imbedding map $f: S^1 \to \Sigma'$ with

$$f((t)) = (f^1(t), \cdots, f^n(t)) = (\varepsilon_1, \cdots, \varepsilon_k e^{it}, \cdots, \varepsilon_n) ,$$

where $(\varepsilon_1, \cdots, \varepsilon_k e^{it}, \cdots, \varepsilon_n)$ satisfies the conditions $a_{i1}z_1 + \cdots + a_{in}z_n = 0 \ (i = 1, \cdots, n-2)$.

The set $\Lambda^{-1}(\xi) \cap \partial N(S_i, \varepsilon_i) \ (\xi \in S^1)$ consists of a union of circles, where $\partial N(S_i, \varepsilon)$ denotes the boundary of ε-tubular neighborhood of the link S_i. We assume that the imbedding maps $g_{is}: S^1 \to \Sigma'$ denotes these circles, where $s = 1, 2, \cdots, d$, $i = 1, \cdots, n$ and the number d means the cardinal number of the above circles. Let θ_i denote the parameter of the i-th component S_i of the multi-link $L(\underline{m})$ defined by the imbedding map $\theta_i: S^1 \to \Sigma$ with $\theta_i(0) = \theta_i(2\pi)$. By using this parameter θ_i, we can construct a new circle S^* on $\partial N(S_i, \varepsilon_i)$ which is homologous to S_i in Σ'. That is, we consider two points $g_{is}(0)$ and $g_{is}(t_0)$ which are contained in the meridian circle at the point $\theta_i(0)$ of S_i. (Here the circle $g_{is}(S^1)$ firstly intersects to this meridian circle at the point $g_{is}(t_0)$ after starting from the point $g_{is}(0)$.) Take an arc L_s^i by joining above two points in the meridian circle and a subarc A_s^i which joins the points $g_{is}(0)$ and $g_{is}(t_0)$ in the circle $g_{is}(S^1)$. By combining L_s^i and A_s^i at the two points $g_{is}(0)$ and $g_{is}(t_0)$, the circle S^* is constructed. Since the circle S^* is homologous to S_i and $\Lambda(g_{is}(S^1)) = \Lambda_1^{m_1}\Lambda_2^{m_2} \cdots \Lambda_n^{m_n}(g_{is}(S^1)) = \xi$, we see that

$$\{\arg \Lambda_i^{m_i}(g_{is}(t_0)) - \arg \Lambda_i^{m_i}(g_{is}(0))\}/2\pi$$
$$= \{m_i(\arg(g_{is}^i(t_0)/|g_{is}^i(t_0)|) - \arg(g_{is}^i(0)/|g_{is}^i(0)|))\}/2\pi$$
$$= -m_1 \operatorname{link}(S_1, S^*) - \cdots - m_{i-1} \operatorname{link}(S_{i-1}, S^*)$$

$$-m_{i+1}\,\mathrm{link}(S_{i+1}, S^*)-\cdots-m_n\,\mathrm{link}(S_n, S^*)$$
$$=-m_1\,\mathrm{link}(S_1, S_i)-\cdots-m_{i-1}\,\mathrm{link}(S_{i-1}, S_i)$$
$$-m_{i+1}\,\mathrm{link}(S_{i+1}, S_i)-\cdots-m_n\,\mathrm{link}\,(S_n, S_i)\,.$$

Thus

$$\{\arg \Lambda_i(g_{is}(t_0))-\arg \Lambda_i(g_{is}(0))\}/2\pi$$
$$=-\{m_1\,\mathrm{link}(S_1, S_i)+\cdots+m_n\,\mathrm{link}(S_n,\,S_i)\}/m_i\,.$$

Now we see that $\Lambda^{-1}(\xi)\cap\partial N(S_i,\,\varepsilon)$ are configurated by the d-parallel $(\alpha,\,\beta)$ toral link, where $\alpha=-(m_1\,\mathrm{link}(S_1, S_i)+\cdots+m_n\,\mathrm{link}(S_n, S_i))/d$, $\beta=m_i/d$ and $d=\mathrm{G.C.D.}$ $(m_i, m_1\,\mathrm{link}(S_1, S_i)+\cdots+m_n\,\mathrm{link}(S_n, S_i))$. Thus $\Lambda^{-1}(\xi)$ is the Seifert surface of a multi-link $L(\underline{m})$ (see the definition of the Seifert surface of multi-links [8]). Since the S^1-action on Σ' is given by $t(Z_1,\cdots,Z_n)=(t^{q_1}Z_1, t^{q_2}Z_2,\cdots,t^{q_n}Z_n)$, we have $\Lambda(tZ)= t^{q_1 m_1+q_2 m_2+\cdots+q_n m_n}\Lambda(Z)=t^l\Lambda(Z)$.

Assume first that $l\neq 0$. Then the fibers of Λ are transverse to the S^1-action on Σ', so Λ is a fibration. Moreover, a typical fiber F of Λ meets each non-singular orbit of S^1-action on Σ' in $|\underline{m}(S_{k+1})|=|l|$ points and meets the singular orbit S_j for $n<j<k$ in $|\underline{m}(S_j)|=|l/a_j|$ points. Thus F is an $|l|$-fold branched cover of $F'=\Sigma'/S^1$ branched over $k-n$ points with branch-indices $a_{n+1},\cdots,a_k$. Since F' is an n-fold punctured sphere, the formula for the Euler characteristic of branched cover gives

$$\chi(F)=|l|(\chi(F')-\sum 1)+\sum|l|/a_j$$
$$=|l|(2-n-\sum(a_j-1)/a_j)=|l|(2-k+\sum 1/a_j)\,.$$

Also, the Seifert surface is a fiber of a fibration Λ. Hence F is a minimal Seifert surface (see Proposition 4.1 in [8]), and that $\|\underline{m}\|=\chi_-(F)=|l|(k-2-\sum 1/a_j)$ hold. Now if $l=0$, then the fibers of Λ are the union of S^1-orbits. And if an orientable surface has a non-singular flow (or a codimension one foliation), then the surface is an annulus. That is, any non-singular fiber F of Λ is a union of annuli. Hence $\chi_-(F)=0$ and we have $\|\underline{m}\|=0$.

Suppose that the intersections of the separatrices and a 3-sphere are a reducible link. When we compute the Thurston norm of this link by using its splice diagram, it requires that the diagram is decomposed so that each connected component represents an irreducible link. The next lemma shows that every splice diagram representing a reducible link satisfies this condition.

LEMMA 5. *Let L be a reducible graph link in S^3 and Γ_L be a splice diagram which represents the link L. Suppose Γ_L is connected and has the arrowhead vertices $v_1,\cdots,v_n$ and the remaining vertices $v_{n+1},\cdots,v_k$. Then, Γ_L has at least one vertex v such that $v=v_j$ for some j with $n+1\leq j\leq k$, and $(l_{1j},\cdots,l_{nj})=(0,\cdots,0)$. (We call v a zero vertex.)*

Moreover, among zero vertices, there is a vertex at which the diagram is decomposed

into a disconnected splice diagram as in Figure 12(a) *or* (b) *where all connected component represent irreducible links in* S^3 *and* Γ_0 *contains no arrowheads.*
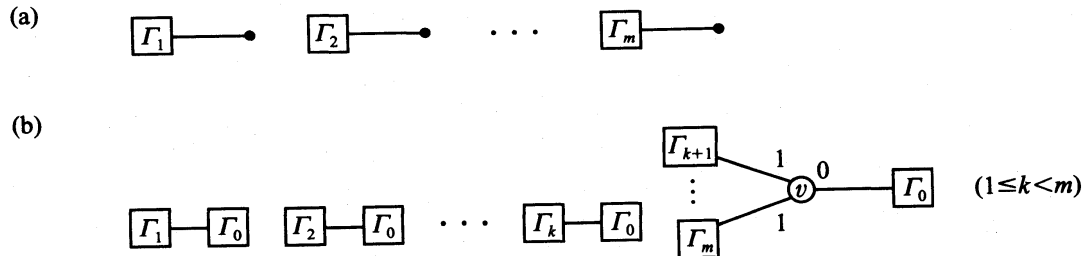
(a)

(b)

$(1 \leq k < m)$

FIGURE 12

PROOF. Let v_i $(i = 1, \cdots, n)$ represent the i-th component S_i of the link L and let $X_1 \cup \cdots \cup X_m$ be the finest partition of $\{v_1, \cdots, v_n\}$ for which $\mathrm{link}(S_i, S_j) = 0$ whenever v_i and v_j belong to distinct X_k's. Here we have $m \geq 2$ since L is a reducible link. If Γ_i is the smallest connected subgraph of Γ_L containing X_i $(i = 1, \cdots, m)$, then Γ_i is irreducible. Also Γ_i is disjoint from Γ_j for $i \neq j$. Then, by Theorem 10.1 in [8], the path in Γ_L connecting Γ_i to Γ_j must pass through a vertex v which has an adjacent edge of weight 0. Define Γ_0 to be the largest connected subgraph of Γ_L which is joined to the vertex v through an edge of weight 0. If Γ_0 contains an arrowhead, then the path from v to this arrowhead passes through a vertex of the same type as v. But the subgraph Γ_0 for this vertex is smaller than the former one. Thus if we choose our vertex v with Γ_0 as small as possible, Γ_0 will contain no arrowheads. At this stage, $v = v_j$ for some j with $n + 1 \leq j \leq k$ and v_j satisfies $l_{1j} = \cdots = l_{nj} = 0$, and Γ_0 contains no zero vertices. We see that the diagram Γ_L is written as follows:
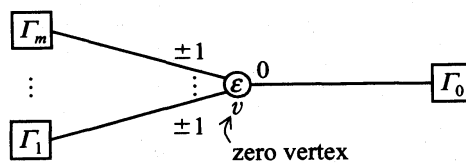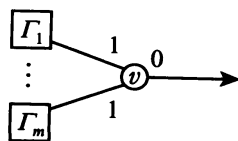
FIGURE 13

where Γ_i $(i = 1, \cdots, m)$ represent irreducible links.

First we assume that $\boxed{\Gamma_0} \mapsto$ represents a trivial knot. Then we see that the diagram Γ_L is decomposed as in Figure 12 (a) by using the operation 2) in Definition 8. So we suppose that the subgraph $\boxed{\Gamma_0} \mapsto$ represents a non-trivial knot. Now we consider the torus corresponding to the cut point on the edge which connects v to Γ_0 in the graph Γ_L. We deal with the link in a 3-sphere and every embedded torus in a 3-sphere bounds a solid torus in one side of it. Also the graph defined by Γ_0 represents a non-trivial knot by our assumption. Thus we can assume that the above torus bounds the solid torus in the side which contains a link represented by

(which we refer to as Γ^*). Let us show this situation in Figure 14.
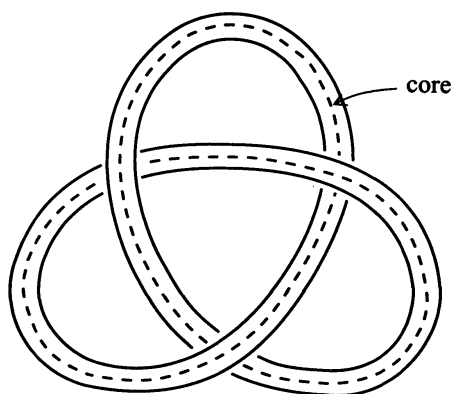

FIGURE 14

The core of the knotted torus in Figure 14 defines a non-trivial knot represented by $\boxed{\Gamma_0}\mapsto$ and we see that the link represented by Γ^* is spliced to $\boxed{\Gamma_0}\mapsto$ along this core of the solid torus. If there exists a 2-sphere in this 3-sphere which separates all link components represented by some Γ_j from others, then the diagram Γ_L is decomposed into the diagram $\boxed{\Gamma_0}\!\!-\!\!\boxed{\Gamma_j}$ which represents an irreducible link and the remaining diagram
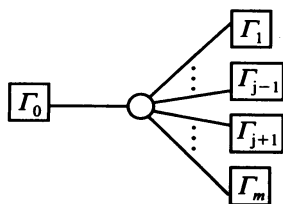
since the diagram Γ_0 has no zero vertices by our construction. We repeat this operation to the latter diagram till *its* remaining diagram represents an irreducible link. Eventually, after changing the indices of the Γ_i's if necessary, the diagram Γ_L decomposes into several diagrams as in Figure 12 (b), each of which represents an irreducible link. This completes the proof. (It can be also shown that a diagram of the form (b) cannot be reduced to a diagram of the form (a).)

REMARK. The splice diagram which has a zero vertex is not always decomposed at the vertex, because it may represent an irreducible link. (See Figure 15.)
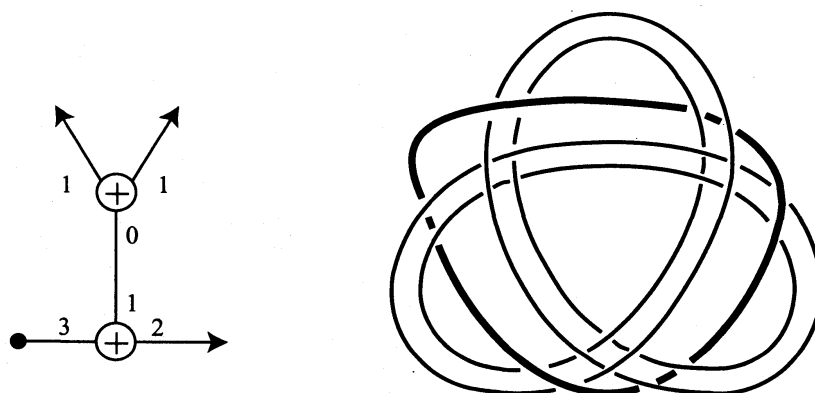
FIGURE 15. The diagram on the left which has a zero vertex represents the irreducible link on the right.

4. Proof of Theorem A and Theorem B.

In this section, we give the proof of main theorems.

PROOF OF THEOREM A. Let S_Z (resp. $S_{Z'}$) be the set of separatrices of the vector field Z (resp. Z'). The separatrices are analytic varieties by Theorem 2, and the arrowhead vertices in the plumbing diagram P_Z (resp. $P_{Z'}$) represent the leaves of F_Z (resp. $F_{Z'}$). These leaves are contained in S_Z (resp. $S_{Z'}$) before desingularizations of the isolated singularity $o \in \mathbb{C}^2$. By Lemma 1 and Lemma 2 P_Z (resp. $P_{Z'}$) is a tree, and the determinant of the intersection form $A(P_Z)$ (resp. $A(P_{Z'})$) induced from P_Z (resp. $P_{Z'}$) is ± 1. Thus we can apply the technique of Neumann to the case of a plane curve and transform the plumbing diagram to a certain type of splice diagram (see [8]). Here we state this technique.

Step 1. The underlying graph of the splice diagram Γ is obtained from the plumbing diagram P by replacing each maximal chain as in Figure 16 by a single edge. All nodes are weighted (or of an orientation weight) $+1$ (see [8] for the definition of a weight of node).
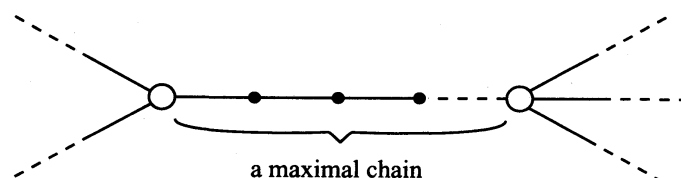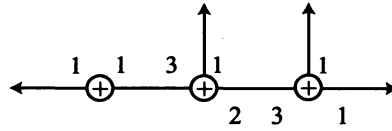

a maximal chain

FIGURE 16

Step 2. The weight at the end of an edge of Γ is $\det(-A(P_1))$ where P_1 is the subgraph of P cut off by the corresponding edge of P and $A(P_1)$ is the intersection form of the plumbing diagram P_1. If P_1 is a single arrowhead, we define $\det(-A(P_1)) = 1$.

For example, the plumbing diagam in Example 1 (see Figure 1) transforms to the splice diagram

by performing Step 1 and Step 2 (see the proof of Theorem 5.1 [14], Theorem 20.1 [8] and Lemma 20.2 [8]).

Now we return to the proof of Theorem A. If Z and Z' are topologically conjugate, then S_Z and $S_{Z'}$ have isomorphic desingularizations. Thus S_Z and $S_{Z'}$ have isomorphic plumbing diagrams. If the separatrices S_Z are desingularized, then the vector field Z is also desingularized by Theorem 2. Thus the final resolution pictures of S_Z and Z are isomorphic. So the plumbing diagrams of S_Z and Z are isomorphic. Since the Milnor number is invariant up to topological equivalence, we obtain that Z' is a generalized curve by Proposition 2 and Theorem 4. Then $S_{Z'}$ and Z' have isomorphic de-singularizations, and we can define the plumbing diagram of Z'. Also $S_{Z'}$ and Z' have isomorphic plumbing diagrams. Hence both plumbing diagrams P_Z and $P_{Z'}$ are isomorphic, and the self-intersection numbers are equal for each corresponding vertices of Z and Z'. Thus applying the above Step 1 and Step 2 to these plumbing diagrams P_Z and $P_{Z'}$, we obtain two isomorphic splice diagrams Γ_Z and $\Gamma_{Z'}$.

Now we assume that Γ_Z has the arrowhead vertices $V_1, \cdots, V_n$ and non-arrowhead vertices $V_{n+1}, V_{n+2}, \cdots, V_k$. Since Γ_Z and $\Gamma_{Z'}$ are isomorphic, two diagrams have the same number of arrowhead vertices and non-arrowhead vertices. By renumbering the vertices of $\Gamma_{Z'}$, we can assume that the i-th vertex of Γ_Z corresponds to the i-th one of $\Gamma_{Z'}$ under the above graph isomorphism. The multiplicities of all arrowhead vertices of Z and Z' are one. Computing Alexander polynomials of L_Z and $L_{Z'}$ from the splice diagrams Γ_Z and $\Gamma_{Z'}$ by Theorem 12.1 of [8], we have

$$\prod_{j=n+1}^{k} (t_1^{l_{1j}} t_2^{l_{2j}} t_3^{l_{3j}} \cdots t_n^{l_{nj}} - 1)^{\delta_j - 2} \qquad \text{(if } n \geq 2\text{)} .$$

If the splice diagram contains only one arrowhead vertex, the Alexander polynomial is given by

$$(t_1 - 1) \prod_{j=2}^{k} (t_1^{l_{1j}} - 1)^{\delta_j - 2} .$$

In the case that $n \geq 2$, we get the one-variable Alexander polynomial by specializing the above polynomial at $t_i = t$ and multiplying by $t - 1$ (Proposition 5.1 in [8]). So this Alexander polynomial does not depend on the indices of vertices of Γ_Z. The numbers of non-invariant vertices of P_Z and $P_{Z'}$ are equal, since Z and Z' have isomorphic desingularizations. Thus if Z and Z' are topologically equivalent, then the pair (Δ_{r_Z}, n_Z)

coincides with $(\Delta_{r_{Z'}}, n_{Z'})$.

We also show the set of n-variable Alexander polynomials defined below is a topological invariant. We will state this fact in the next corollary.

Suppose that the splice diagram Γ_Z of a vector field Z has k vertices ($k \geq 3$) including n arrowhead vertices ($n \geq 2$). The set of n-variable Alexander polynomials of Z is defined by

$$\left\{ \Delta_Z^\sigma(t_1, t_2, \cdots, t_n) = \prod_{i=n+1}^{k} (t_1^{l_{\sigma(1)i}} \cdots t_n^{l_{\sigma(n)i}} - 1) \,\middle|\, \sigma \in S_n \right\},$$

where S_n means a symmetric group of which order is $n!$ and l_{ji} denotes the linking number for the j-th arrowhead vertex and the i-th non-arrowhead vertex. We firstly label the n arrowhead vertices of Γ_Z integers $1, 2, \cdots$ and n. We can choose this numbering arbitrarily, because the set of Alexander polynomials does not depend on the choice of the numbering, i.e., the Alexander polynomial of the first numbering $\Delta_Z(t_1 \cdots t_n) = \prod_{i=n+1}^{k} (t_1^{l_{1i}} t_2^{l_{2i}} \cdots t_n^{l_{ni}} - 1)$ alters to $\Delta_Z^\sigma(t_1 \cdots t_n) = \prod_{i=n+1}^{k} (t_1^{l_{\sigma(1)i}} t_2^{l_{\sigma(2)i}} \cdots t_n^{l_{\sigma(n)i}} - 1)$ by changing the numbering for the arrowheads.

COROLLARY 1. *Let Z and Z' be as in Theorem A, and Γ_Z be the splice diagram of Z which has k vertices including n arrowhead vertices ($n \geq 2$). Then the set of n-variable Alexander polynomials of Z' coincides with the one for Z.*

PROOF. Since Z is topologically equivalent to Z', the splice diagram of Z' agrees with Γ_Z. Then the Alexander polynomials of Z' is defined by $\prod (t_1^{l_{\sigma(1)i}} t_2^{l_{\sigma(2)i}} \cdots t_n^{l_{\sigma(n)i}} - 1)$ ($^\exists \sigma \in S_n$) for a certain numbering of arrowhead vertices of $\Gamma_{Z'}$, and it belongs to the set of n-variable Alexander polynomials of Z. Thus the set for Z' coincides with the one for Z.

PROOF OF THEOREM B. Since the generalized curves Z and Z' are topologically equivalent, they induce the same splice diagrams Γ_Z and $\Gamma_{Z'}$ through the same argument as in the proof of Theorem A. Note that this process includes Steps 1 and 2 in the proof of Theorem A. Then a leaf preserving homeomorphism h defined on an open neighborhood of $o \in \mathbf{C}^2$ induces a graph isomorphism between these splice diagrams Γ_Z and $\Gamma_{Z'}$, and multiplicities are one for all arrowhead vertices of Γ_Z and $\Gamma_{Z'}$. Let L_Z (resp. $L_{Z'}$) be a link in S^3 represented by Γ_Z (resp. $\Gamma_{Z'}$). If L_Z is irreducible, then $L_{Z'}$ is also irreducible. Let m_Z (resp. $m_{Z'}$) be a cohomology class in $H^1(S^3 - L_Z)$ (resp. $H^1(S^3 - L_{Z'})$) which represents the link L_Z (resp. $L_{Z'}$). Since the multiplicities take the same values on the corresponding arrowhead vertices of the diagrams Γ_Z and $\Gamma_{Z'}$, we have $\|m_Z\| = \|m_{Z'}\|$ by Theorem 5. If L_Z is reducible, then $L_{Z'}$ is also reducible. Since the diagrams Γ_Z and $\Gamma_{Z'}$ are isomorphic, both Γ_Z and $\Gamma_{Z'}$ are decomposed into the isomorphic splice diagrams by Lemma 5. We can assume that all of these decomposed splice diagrams are irreducible. Suppose that Γ_Z^i (resp. $\Gamma_{Z'}^i$) ($i = 1, \cdots, m$) are the decomposed splice diagrams of Γ_Z (resp. $\Gamma_{Z'}$), and that m_Z^i ($i = 1, \cdots, m$) (resp. $m_{Z'}^i$) is a cohomology class in $H^1(S^3 - L_Z)$ (resp. $H^1(S^3 - L_{Z'})$) representing the link L_Z^i (resp. $L_{Z'}^i$). Then $\|m_Z^i\| = \|m_{Z'}^i\|$

$(i = 1, \cdots, m)$ and, by the additivity of the Thurston norm, we have $\|m\| = \|m'\|$.

REMARK. If the homeomorphism which gives the topological equivalence between Z and Z' is an orientation preserving map, the assumption that all vertex weights of $\Gamma_{Z'}$ are $+1$ in the proofs of Theorems A and B can be removed. We need here only the assumption for Γ_Z. The orientation preserving and leaf preserving homeomorphism may change the orientations of all link components simultaneously. Hence it may change the signs of all vertex weights simultaneously. Thus we obtain the invariants considering the sign of vertex weights of the splice diagrams. In fact, take the form of the Alexander polynomial $A(t_1 \cdots t_n)$ in Theorem A, and then Alexander polynomial $A(t, t^{-1}) \pmod{\pm t^N}$ for some integer N is invariant under such a homeomorphism, and so is the Thurston norm in Theorem B.

We list all the Thurston norms and Alexander polynomials of the diagrams in Examples 1 to 4.

	Example 1	Example 2	Example 3	Example 4
Minimal splice diagram				
(Δ, n_z)	$((t-1)(t^{10}-1)(t^{14}-1), 1)$	$(t^2-t+1, 0)$	$(1, 1)$	$(t-1, 0)$
Thurston norm	24	1	0	0

The next proposition asserts that the Δ_Z in the pair (Δ_Z, n_Z) of Theorem A is not equal to $\varnothing$, except for certain special vector fields.

PROPOSITION 1. *Suppose that Z is a holomorphic vector field defined on a neighborhood of the origin $o \in \mathbf{C}^2$. Assume further that Z is not topologically equivalent to the following vector field;*

$$Z_0(z_1, z_2) = z_1 \frac{\partial}{\partial z_1} + z_2 \frac{\partial}{\partial z_2}, \qquad (z_1, z_2) \in \mathbf{C}^2 .$$

Then the splice diagram Γ_Z induced by Z has at least one arrowhead vertex.

PROOF. If Z has no zero eigenvalues, Z is topologically equivalent to one of the following (see [4] and [6]).

(1) $Z_1(z_1, z_2) = z_1(\lambda_1 + a_1(z_1, z_2))\partial/\partial z_1 + z_2(\lambda_2 + a_2(z_1, z_2))\partial/\partial z_2$ where $\lambda_1/\lambda_2 \in \mathbf{Q}_+$.

(2) $Z_2(z_1, z_2) = (\lambda_1 z_1 + az_2^n)\partial/\partial z_1 + (\lambda_2 z_2)\partial/\partial z_2$, where $\lambda_1 = n\lambda_2$ and $a \neq 0$.

(3) $Z_3(z_1, z_2) = pz_1\partial/\partial z_1 + z_2\partial/\partial z_2$ (or $z_1\partial/\partial z_1 + pz_2\partial/\partial z_2$) where $p \in \mathbf{N}$. Here p is not equal to 1 by the assumption.

(4) $Z_4(z_1, z_2) = pz_1\partial/\partial z_1 + qz_2\partial/\partial z_2$ where $p, q \in \mathbf{N}$, G.C.D.$(p, q) = 1$ and both p and q are not equal to 1 by the assumption.

We assume that Z is topologically equivalent to Z_1 which has two invariant curves defined by $z_i = 0$ $(i = 1, 2)$. So the final resolution picture of Z_1 has two arrowhead lines. Then we see the splice diagram Γ_{Z_1} derived from Z_1 has two arrowhead vertices, and so does Γ_Z (see the proof of Theorem A).

We assume that Z is equivalent to Z_2. We can directly check that Z_2 has only one integral curve passing through the origin by using the following differential equations; $dz_1/dt = \lambda_1 z_1 + az_2^n$, $dz_2/dt = \lambda_2 z_2$. Thus Γ_{Z_2} has one arrowhead vertex, and so does Γ_Z.

Next we consider the case (3). The vector field Z_3 has the following final resolution picture. Thus the splice diagram Γ_{Z_3} has only one arrowhead vertex, and so does Γ_Z (cf. Example 3).

$p-1 \quad p \quad p-3 \quad p-2$ $\qquad\qquad\qquad\qquad$ 1
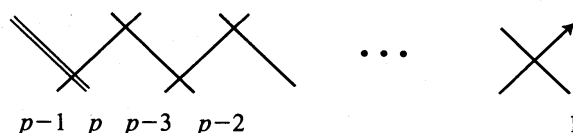
The final resolution picture of Z of the case (4) has one arrowhead line, since this case is similar to the case (3). Then Γ_Z of this case has only one arrowhead vertex (see the following diagram).
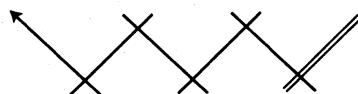
If Z has at most one non-zero eigenvalue, we can check that the desingularization (U_Z, π_Z, P_Z, F_Z) has at least one leaf which transversely intersects to an invariant component of P_Z by using the same methods as in the proof of the main theorem in [5]. Thus the splice diagram Γ_Z has arrowhead vertex. Now we obtain the desired results.

REMARK.   If Z is topologically equivalent to $Z_0 = z_1 \partial/\partial z_1 + z_2 \partial/\partial z_2$, we see that the pair (Δ_Z, n_Z) is equal to $(\varnothing, 1)$.

5.   A multiple link as a topological invariant near an isolated singularity.

Suppose that a vector field Z is a nondegenerate generalized curve. Then the set of separatrices of Z represents an analytic curve $f(x, y) = 0$ in $\mathbf{C}^2$ with the isolated singularity $o \in \mathbf{C}^2$. A vector field Z and its separatrices $f(x, y) = 0$ have isomorphic desingularizations by Theorem 3. If analytic curves are desingularized, we can define the multiplicities on every arrowhead vertices (see [8]). The arrowhead vertices of the plumbing diagram of separatrices $f(x, y) = 0$ correspond to those of the plumbing diagram of the vector field, because the separatrices $f(x, y) = 0$ are leaves of F_Z passing through the origin $o \in \mathbf{C}^2$. Thus the multiplicities on the arrowhead vertices of a plumbing diagram is defined. We call the plumbing diagram which has arrowhead vertices with

multiplicity a *weighted plumbing diagram*. Using the weighted plumbing diagram which induces the one-variable Alexander polynomials, we get the splice diagram furnishing arrowhead vertices with multiplicity. Also we have the Thurston norm of a multi-link $L_Z(m_1, \cdots, m_n)$, where the number $m_i \in \mathbf{Z}$ defines the multiplicity of the link component S_i of L_Z corresponding to the arrowhead vertex of a splice diagram of the vector field ($i = 1, \cdots, n$). Now we have the following propositions for Alexander polynomials and Thurston norms.

PROPOSITION 2.   *In the case of a nondegenerate generalized curve, one-variable Alexander polynomial of the splice diagram induced from a weighted plumbing diagram is a topological invariant near the isolated singularity $o \in \mathbf{C}^2$.*

PROOF.   Suppose that Z and Z' are topologically equivalent and that Z is a nondegenerate generalized curve. Then the both separatrices have isomorphic desingularizations. By using the same arguments as in the proof of Theorem A, we see that the plumbing diagram of Z is isomorphic to that of Z', which also coincides with those of separatrices of Z and Z'. The multiplicity of arrowhead vertices of separatrices is invariant up to sign under a map which gives the topological equivalence between Z and Z'. Hence the two splice diagrams with the weighted arrowhead vertices are equivalent if we first put the $+1$ weight on all the arrowhead vertices of both splice diagrams. The Alexander polynomial induced from the splice diagram of which all arrowhead vertices have multiplicity one is a topological invariant by Theorem A. Also the one-variable Alexander polynomials are given by the substitution $t_i \to t^{m_i}$ in $\Delta_{\Gamma_Z}(t_1, \cdots, t_n)$, where the number m_i is the multiplicity of the link component S_i corresponding to an arrowhead vertex of the splice diagram Γ_Z, and then multiplying the polynomial $t^d - 1$ ($d = \text{G.C.D.}(m_1, m_2, \cdots, m_n)$). Since the multiplicities of analytic curves are positive, all of the multiplicities of arrowhead vertices are positive. Thus one-variable Alexander polynomials $\Delta_{\Gamma_Z}(t)$ are topological invariant.

PROPOSITION 3.   *The Thurston norm of multiple link $L(m_1, \cdots, m_n)$ induced by the splice diagram of a nondegenerate generalized curve is a topological invariant near an isolated singularity.*

The proof is similar to that of Proposition 2. So we omit the proof.

For the case of the Hamiltonian systems defined in an open neighborhood of the origin $o \in \mathbf{C}^2$, it is easy to know its separatrices. Thus we can obtain the Thurston norm and the one-variable Alexander polynomial concretely. For example, the equation

$$\dot{x} = -x^{11} - 6x^8 y^2 + 8x^6 y^3 - 5x^5 y^4 - 8y^7$$
$$\dot{y} = 12x^{11} + 16x^7 y^3 + 11x^{10} y - 12x^5 y^4 + 5x^4 y^5$$

is a Hamiltonian system which are defined by an analytic curve $f(x, y) = (x^6 - y^4)^2 + x^5 y(x^3 + y^2)^2 = 0$. The splice diagram with weighted arrowhead vertices for this vector

field is as follows. (The numbers (1) and (2) mean the multiplicities of arrowhead vertices.)
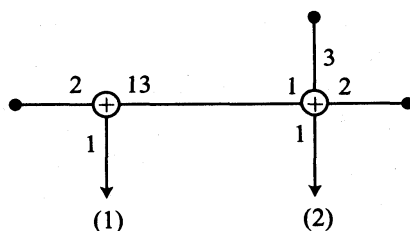

FIGURE 17

The one-variable Alexander polynomial is $(t-1)(t^{12}+1)(t^{25}+1)(t^{16}+t^8+1)$ since the ordinary Alexander polynomial is given by

$$\Delta_{\Gamma_{z_f}} = (t_1^{13}t_2^{12}-1)^{-1}(t_1^{24}t_2^{24}-1)(t_1^{12}t_2^{12}-1)^2(t_1^4t_2^4-1)^{-1}(t_1^6t_2^6-1)^{-1}.$$

And the Thurston norm is 53 (which is obtained by using Theorem 5). The following two corollaries are direct consequences of Propositions 2 and 3.

COROLLARY 2. *Suppose that Z_f and $Z_{f'}$ are Hamiltonian systems. If Z_f and $Z_{f'}$ are topologically equivalent, then the Thurston norm of Z_f is equal to that of $Z_{f'}$.*

COROLLARY 3. *Let Z_f and $Z_{f'}$ be as above. If Z_f and $Z_{f'}$ are topologically equivalent, then the one-variable Alexander polynomial of Z_f is equal to that of $Z_{f'}$.*

If a vector field Z is the non-degenerate generalized curve of which separatrices are defined by $f=0$, then the Milnor number $\mu(Z)$ for Z is equal to the Milnor number $\mu(Z_f)$ for the Hamiltonian system defined by the equation $\dot{x}=-\partial f/\partial y$, $\dot{y}=\partial f/\partial x$ (see [4]). On the other hand, the foliation of the Hamiltonian Z_f around the isolated singularity is topologically equivalent to the Milnor fibration defined by $f=c$, $0\leq|c|\leq\varepsilon$, where ε is a sufficiently small real number (see [4]). Thus the Milnor number $\mu(Z_f)$ is equal to the Milnor number of the analytic curve $f=0$. Hence the Thurston norm of Z_f is equal to $\mu(Z_f)-1$. Thus the Thurston norm in Proposition 3 is equal to $\mu(Z)-1$ for the cases of nondegenerate generalized curves.

Now, it seems to be hard to calculate the multiplicity $(m_1,\cdots,m_n)$ of arrowhead vertices, unless a given vector field is integrable as Hamiltonian systems. And yet we can obtain the multiplicity for certain vector fields. For the purpose it is effective to observe the holonomy of the vector field around a singularity. We will discuss this method in the forthcoming paper [18].

References

[1] I. BENDIXSON, Sur les points singuliers d'une équation différentielle linéaire, Ofv. Kongl. Ventenskaps Akademiens Forhandlinger **148** (1895), 81–89.

[2] C. CAMACHO, On the local structure of conformal mappings and holomorphic vector fields in C^2, Astérisque 59–60 (1978), 83–94.

[3] C. CAMACHO, C. KUIPER and J. PALIS, The topology of holomorphic flows with singularity, Publ. Math. IHES 48 (1978), 5–38.

[4] C. CAMACHO, A. L. NETO and P. SAD, Topological invariants and equidesingularization for holomorphic vector fields, J. Differential Geometry 20 (1984), 143–174.

[5] C. CAMACHO and P. SAD, Invariant varieties through singularities of holomorphic vector fields, Ann. of Math. 115 (1982), 579–595.

[6] C. CAMACHO and P. SAD, Topological classification and bifurcations of holomorphic flows with resonances in C^2, Invent. Math. 67 (1982), 447–472.

[7] H. DULAC, Recherches sur les points singularities de équations différentielles, J. Ecole Polytechnique 2 (1904), 1–125.

[8] D. EISENBUD and W. D. NEUMANN, Three-Dimensional Link Theory and Invariants of Plane Curve Singularities, Ann. Math. Studies 110 (1986), Princeton Univ. Press.

[9] F. HIRZEBRUCH, W. D. NEUMANN and S. S. KOH, Differentiable manifolds and quadratic forms, Lecture Notes Pure Appl. Math. 4 (1971), Marcel Dekker.

[10] S. LEFSCHETZ, On a theorem of Bendixson, J. Differential Equations 4 (1968), 66–101.

[11] MATTEI and R. MOUSSU, Holonomie et integrales premières, Ann. Sci. Ecole Norm. Sup. (4) 13 (1980), 469–523.

[12] J. MILNOR, Singular points of complex hypersurfaces, Ann. Math. Studies 61 (1962), Princeton Univ. Press.

[13] A. L. NETO, Construction of singular holomorphic vector fields and foliations in dimension two, J. Differential Geometry 26 (1987), 1–31.

[14] W. D. NEUMANN, A Calculus for plumbing applied to the topology of complex surface singularities and degenerating complex curves, Trans. Amer. Math. Soc. 268 (1981), 299–344.

[15] W. D. NEUMANN, Complex algebraic plane curves via their links at infinity, Invent. Math. 98 (1989), 445–489.

[16] W. D. NEUMANN, On the topology of curves in complex surfaces, Topological Methods in Algebraic Transformation Groups, Proc. Conf. Rutgers Univ., Progress in Math. 80 (1989), 117–133.

[17] W. D. NEUMANN and L. RUDOLPH, Difference index of vector fields and the enhanced Milnor number, Topology 29 (1990), 83–100.

[18] N. OKA, Graph link invariants of isolated singularities of holomorphic vector fields in C^2 II, Tokyo J. Math. 19 (1996), 317–329.

[19] A. SEIDENBERG, Reduction of singularities of the differentiable equation $AdY = BdX$, Amer. J. Math. 90 (1968), 248–269.

[20] O. ZARISKI, On the topology of algebroid singularities, Amer. J. Math. 54 (1932), 453–465.

Present Address:
SHIMOTAKAIDO 3–32–7, SUGINAMI-KU, TOKYO, 168 JAPAN.